Journal of Engineering and Sustainable Development
Vol. 29, No. 03, May 2025
https://jeasd.uomustansiriyah.edu.iq/index.php/jeasd
ISSN 2520-0917
Research Article
https://doi.org/10.31272/jeasd.2012

Fabrication of the Polyvinylidene fluoride (PVDF) Nanofibers Membranes Via Electrospinning Technique for Oil Removal

Thamer Diwan[1*], Zaidun N. Abudi[2], Mustafa H. Al-Furaiji[3], Rouhollah Y. Farsani[4]

[1]Technical Directorate, Ministry of Environment, Baghdad, Iraq
[2]Environmental Engineering Department, College of Engineering, Mustansiriyah University, Baghdad, Iraq
[3]Water, Environment, and Renewable Energy Center, Scientific Research Commission, Ministry of Higher Education and Scientific Research, Baghdad, Iraq
[4]Energy and Environment Research Center, Shahrekord Branch, Islamic Azad University, Shahrekord, Iran

[*]Email: thamerdiwanfdzm@uomustansiriyah.edu.iq

Article Info

Received	**19/03/2023**
Revised	**17/03/2025**
Accepted	**23/03/2025**

Abstract

The treatment of oily wastewater is a challenging and complex task. Their efficiency in removing oil was evaluated in efforts to reach two objectives: increasing permeate flux as well as maximizing oil removal. The surface features of the constructed membranes were examined with a FESEM device, and atomic force microscopy (AFM) was employed to investigate the topography of the substrate surfaces. The water contact angle and wettability were determined using the Contact Angle Measuring Instrument; Porosity was evaluated through a gravimetric method, while the average diameter of the nanofibers was measured with ImageJ software. It was observed that higher concentrations of PVDF/DMF precursor solutions led to an increased average diameter of the nanofibers within the membranes, which is between 0.175 and 0.4 µm. Furthermore, the membranes surfaced exhibited an increase in average surface roughness (Ra) from 0.171 µm to 0.279 µm, while the contact angle increased from 81° to 135°. This demonstrates that the 14% PVDF-based nanofiber membrane had hydrophobic properties. These variations positively affected the membrane's efficiency, as demonstrated by the increase in permeate flux and oil rejection rate, which rose from 58 to 136 LMH and from 85.5 to 96%, respectively, without applying any pressure.

Keywords: Electrospun nanofibers, Oil emulsion, Oil rejection, Permeate flux, Polymeric membrane, Polyvinylidene fluoride polymer.

1. Introduction

Access to clean and safe water is essential for human health and well-being, but it is becoming an increasingly scarce resource due to pollution and overuse. The United Nations estimates that by 2025, half of the world's population will face water shortages; by 2030, the water demand could exceed supply by 40%. In Iraq, water scarcity is a significant issue. Efficient management of wastewater is central to ensuring the sustainability of water resources. It was, however, considered a mere byproduct instead of a valuable resource. If properly treated, wastewater can be reused for various purposes, which helps minimize the contaminants present in water bodies [1].

The use of membrane technology is increasing due to its effectiveness in desalination and wastewater purification. This technique offers several advantages over traditional methods, including a high permeability level for oil-water separation, leading to enhanced separation efficacy and reduced energy usage during the process [2], [3]. Meanwhile, conventional methods used for water purification, such as dissolved air flotation (DAF), ultrasonic separation, skimming, coagulation-flocculation, and gravity processing, are associated with certain drawbacks. These problems can include the following issues: low efficiency in the separation process, considerable energy consumption, additional pollutants, and the need for separation advanced instrumentation [4]. Oils are commonly present in wastewater and come in two main types: free oils and emulsified oils [5]. Conventional methods can remove the free oil portion. Nevertheless, the emulsified and dispersed oil

particles are the most challenging to work with because of their strong stability in the liquid state [6].

Membranes are generally classified into two main types: natural and artificial. Living cells undergo specific natural membranes which serve specialized purposes and are intricately structured. Synthetic membranes, in contrast, are made from specially manufactured materials for separation. They are categorized based on the materials used as either organic (polymeric) or inorganic membranes. Technologies connected to membranes usually depend on organic materials, especially polymers such as polyacrylonitrile, polyvinylidene fluoride, polysulfone, polyethersulfone, polytetrafluoroethylene, and polyamide-imide. This is because they perform very well. These polymers have broad usage in scientific and engineering fields [7].

On the other hand, inorganic membranes are usually made of metals, ceramics, or zeolites, which are standard materials in membrane construction [8]. However, inorganic membranes have some definite problems due to their intricate structural features and more rigid transport processes than polymeric membranes [9]. As a result, polymeric membranes have become increasingly important components of various industries that seek to improve their water treatment technologies [10].

Different contaminants in wastewater, such as oil emulsions, suspended particles, bacteria, cells, viruses, macromolecules, proteins, sub-molecular organic groups, and various ions, can be separated depending on the membrane separation techniques used. This covers the MF (microfiltration) procedure where filters with sizes between 0.1 and 1.0 nm are used [11], ultrafiltration (UF) with pore sizes ranging from 1 to 100 nm, reverse osmosis (RO) along with nanofiltration (NF), which has pores ranging from 0.5 to 5 nm. Additionally, there are different categories of membrane separation processes based on the force driving the separation. The pressure requirements for these processes vary, with MF requiring 0.1 to 2 bar, UF requiring 1 to 10 bar, and NF requiring 5 to 20 bar for separation [12].

For example, electrospinning and phase inversion techniques can be used to manufacture polymeric membranes [13]. The phase inversion method is a controlled technique in which a homogeneous polymeric solution transforms from a liquid to a solid phase [14]. Electrospinning is when a high voltage is applied to a polymeric solution or grilled polymer. It is remarkably economical and flexible for producing continuous fibers with diameters ranging from one nanometer to a micrometer [15]. Many researchers have employed electrospun nanofibers in different fields, such as fabricating separation membranes, tissue engineering, high-performance air filters, and sensors [16]. Electrospinning provides a convenient method for creating nanofibrous substrates with a broad specific area and more than 90% porosity, displaying significant potential in wastewater treatment [17], [18].

This study concentrates on the electrospinning technique of nanofiber membrane fabrication, where poly (vinylidene fluoride) (PVDF) was dissolved in N, N-dimethylformamide (DMF) as a solvent. We chose polyvinylidene fluoride (PVDF) to produce hydrophobic electrospun PVDF-based nanofiber membranes due to its excellent processability and chemical resistance to various substances, including organic solvents, acids, bases, grease, and fat. This is owing to its thermal stability and mechanical strength [19].

The PVDF nanofiber membranes produced via electrospinning are classified as hydrophobic membranes. Using highly porous and hydrophobic nanofiber membranes can help prevent pore wetting and enhance water permeation flux [20]. Hydrophobic electrospun nanofiber membranes are becoming more common in water treatment and have shown superior distillation performance[21]. M. Obaid and their team [22] prepared electrospun membranes of pristine PVDF and PVDF/TEA for oil/water separation. When tested under atmospheric pressure, the pristine PVDF membrane demonstrated a water flux of 273 LMH. They subsequently regulated the water flux solely by relying on the liquid transfer pump to increase the pressure head. Du and colleagues [23] prepared pristine PVDF and PVDF/PVP-TiO2 nanofiber membranes for separating oil-water emulsions. Although the pristine PVDF membrane exhibited no water flux, adding PVP and TiO2 significantly enhanced the water flux, leading to excellent separation efficiency. Venkatesh and their team [24] observed a decrease in water flux for pristine PVDF membranes, but after modification, the flux was found to have improved. The PVDF-modified membranes exhibited excellent separation efficiency for both dye and oil-water emulsions.

This research has succeeded in devising an innovative solution for preparing PVDF electrospun nanofiber membranes and evaluating their performance in oil-water separation.

2. Experimental Procedures and Materials

2.1. Materials

Shanghai Fluorine Chemical Industry, China, provided PVDF powder (FR904), and Thomas Baker (Chemicals) Pvt. Ltd. supplied N, N-Dimethylformamide (DMF) with a molecular weight of 73.1 g/mol. Moreover, Hopkin & Williams Ltd. provided Tween 80. The Midland Iraqi Refining Company provided this study with a hydrocarbon fuel that weighs 175 grams per mole.

2.2. The Combining of Precursors

Three different percentages of polyvinylidene fluoride (PVDF)—10, 12, and 14 wt.%—were added to DMF and stirred magnetically. After 6 hours of stirring at 60°C, a clear and consistent solution was obtained. The solutions were left to sit at room temperature overnight to allow any trapped air bubbles to escape.

2.3. Fabrication of Electrospun Nanofiber Layers

The fabrication of nano-fiber layers by nonwoven means was conducted with the help of an electrospinning machine. The electrospinning device was a custom-made system assembled at the Ministry of Science and Technology's Environment and Water Directorate.

During the electrospinning procedure, the polymer solution was dispensed through a single-use plastic syringe with a capacity of 5 ml and equipped with a 23G specification metal capillary

needle. A controlled dispensing pump secured the syringe, and PVDF/DMF precursor solutions were prepared at varying concentrations of 10, 12, and 14 wt.%, which were later used. The needle tip (positive side) was positioned 17 cm from a rotating metal drum collector (negative side), and a high-voltage power supply (30 KV) was used to create an electrostatic force between them. This force caused the polymer solution to be in motion, and when it was released into an atmosphere, it led to the generation of nanofibers. Meanwhile, the portion that was liquid eventually vaporized. Finally, an arrangement of disorderly and accidentally placed nanofibers was collected on the cylindrical rotating metal drum, which measured 25 × 25 cm.

2.4. Characterization of membranes

The characterization process was conducted via the Inspect F50 by FEI Technologies Incorporation using field emission scanning electron microscopy (FESEM). The membrane samples were analyzed by high-resolution imaging with a voltage of 20 kV. Gold membranes were coated before SEM imaging to improve the surface conductivity.

The mean nanofiber diameter was determined by analyzing twenty images per sample using the software provided by the National Institutes of Health USA, ImageJ [25].

To examine the substrate's surface topography, a high-resolution XE 100 AFM device manufactured by Park Systems in Korea was employed. The specimen was scanned three times in tapping mode, during which the mean surface texture Ra was calculated from the atomic force microscopy system's texture evaluation report.

An assessment of the wettability of the PVDF membranes was performed using a Theta Lite TL-101 (Thailand) device, which measures the contact angle with water. Three different places on the membrane were examined, and the contact angles of water drops were calculated for each membrane sample.

The gravimetric method was used to determine the membrane samples' porosity. An initial lightweight, moisture-free circular membrane specimen with a radius of 1.5 cm was manufactured and further dried (W_{dry}). Then, the sample was immersed in Isopropyl alcohol (IPA) and weighed again (W_{wet}). The porosity (Ɛ) was calculated using the following formula [26]:

$$\varepsilon = \frac{\frac{\mathrm{Wwet} - \mathrm{Wdry}}{\rho\mathrm{IPA}}}{\mathrm{V}} \times 100\ \% \qquad (1)$$

The sample volume is denoted as V, whereas ρIPA is the density of IPA. To ensure accuracy, every membrane was assessed at least three times.

2.5. Performance test for oil removal

The solution was stirred very well after adding 1 gram of kerosene and 0.1 gram of Tween 80 in a beaker of one-liter purified water; an emulsion solution with a concentration of 1 g/L was prepared and achieved stability. The SRH-S Lab emulsifier was utilized to thoroughly blend this formulation for thirty minutes while maintaining room temperature and a speed of 10,000 rpm. The emulsified solution was prepared a day before the experiment to prevent oil droplets from sticking during storage [27]. An oil-in-water measurement was performed on a Vis-722G & UV-9200 spectrophotometer Biotech Engineering Management Co. Ltd that operated with a 1.0 cm quartz cell at a wavelength of 290 nm. The degree of separation of oil is determined using a tangential flowing filtration device which is a type of crossflow filter unit, which is provided in Fig. 1. This system included a feed tank (FT) coupled with a pumping unit (P) and permeates tank (PT), flow meter (F), valves (V1, V2), pressure monitoring gauge (PG) and a custom-built tangential flow filtration unit (CM) were utilized. The filtration unit comprised a Perspex chamber in a box-like configuration, measuring 6 x 12 cm², and contained a membrane segment with an operational surface area of 2.5 x 8 cm². A thin net-like mesh was used to secure the membrane piece in place, reinforced by a rectangular rubber gasket [28].

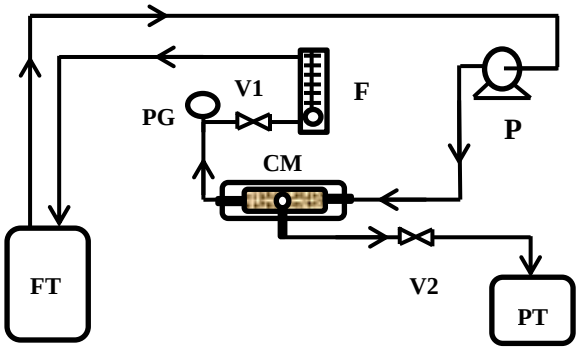

Figure 1. Graphical depiction of the crossflow filtration system implemented in the verified study.

A pump circulated the solution into the filtration chamber while the filtered liquid was collected in a beaker. The time it took to collect a specific fluid volume was measured to determine the permeate flux. Meanwhile, the fluid movement rate and applied force were adjusted using control mechanisms. The measuring instruments individually presented the corresponding values for flow and pressure. The effectiveness of separation of oil emulsion and emulsion flux was checked by volumetric measurement of permeate about time employing the following equation [29]:

$$R\% = \left[1 - \left(\frac{Ct}{Co}\right)\right] \times 100\ \% \qquad (2)$$

$$J = \frac{V}{A \times t} \qquad (3)$$

Where (R %) is the oil rejection percentage, it is calculated using the concentration of oil in the collected water (Ct) and the oil emulsion (Co) in mg/l. The flux of the membrane (J) is in LMH (The flux is defined as the rate of liquid flow that passes through the membrane layer and exits it, often expressed as volume per unit area per unit time. As a result, the flux unit of (L/hr. /m^2) is commonly abbreviated as LMH, while the valid filtration surface area of the membrane (A) is in m^2. The volume of permeate (V) is in liters (L), and the separation time (t) is in hours (h). Each test involved pouring a specific emulsion into the feed tank, and the mean for each system was calculated by analyzing three independent samples.

3. Results and Discussion

3.1. Characterization of membranes

Surface morphologies and pore size distributions of membranes made from different concentrations of PVDF/DMF precursor solution are shown in Fig. 2. Observing the Fiber Formation, we notice that the beads accompany the fibers. The beads are abundant in the 10 wt.% and 12 wt.% PVDF/DMF fibers, whereas in the 14 wt.% PVDF/DMF fibers, a lower bead density is observed, as presented in Fig. 2c. This phenomenon is caused by the presence of beads, which, as the concentration of polymer increases, decreases during the process of electrospinning; when the solution is diluted, both fibers, as well as beads, appear; however, with the rise in the viscosity of the solution, the beads are transformed into high-density fibers [30] and for PVDF/DMF compositions containing 10, 12, and 14 wt.%, the fibers within the membranes had an average diameter of about 175 nm, 270 nm, and 400 nm, respectively.

It should be mentioned that as the concentration of the precursor solution increases, the average fiber diameter of the electrospun nonwoven membranes increases as well. This behavior was also observed in [27], [28]. Moreover, it is important to observe that the fibers' average diameter in the nanostructured membranes was approximately 175 nm, 270 nm, and 400 nm at PVDF/DMF levels of 10, 12, and 14 wt.%, respectively [31],[32].

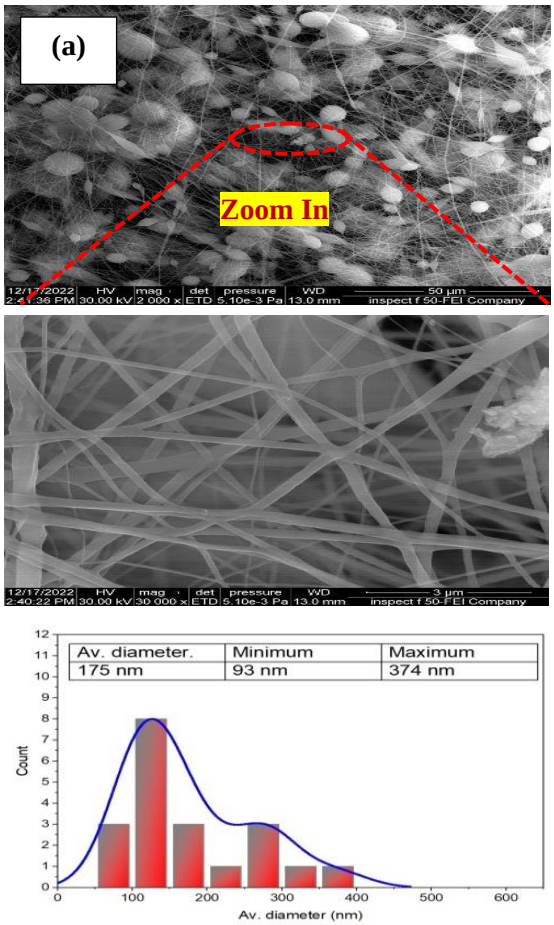

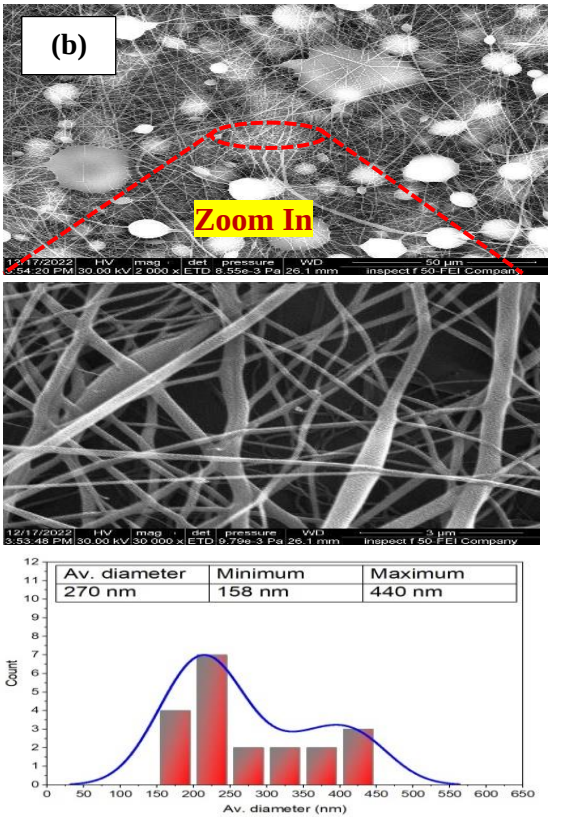

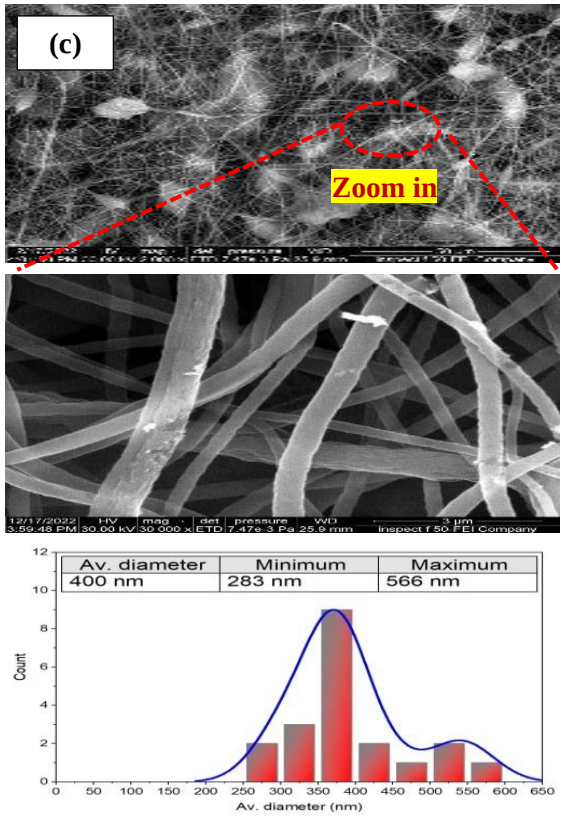

Figure 2. The FE-SEM image shows the different precursor concentrations and corresponding fiber diameters: (a) 10 wt.%, (b) 12 wt.%, and (c) 14 wt.% of a PVDF solution in DMF solvent mixture.

3.2. Topography of membranes

Shown in Fig. 3 are the AFM micrographs, which show how networks of electrospun nanofibers resemble after being fabricated using PVDF/DMF solutions at 10, 12, and 14 wt.%. The images were obtained from a 15 x 15 μm area of interest, yielding an AFM 3D scan showing the nanofibers' surface morphology, height variations, and structure features. When the initial mixture concentration of PVDF in the DMF-based solvent system was increased from 10 wt% to 14 wt%, the membrane surface roughness (Ra) increased from 171 nm to 279 nm. The fiber's structural organization inside the membranes is transparent, and as the concentration of the precursor mixture grows, it is evident that the surface roughness increases.

When the fiber thickness in the membrane increased, surface roughness also increased. This finding is consistent with the results of previous studies, such as [33].

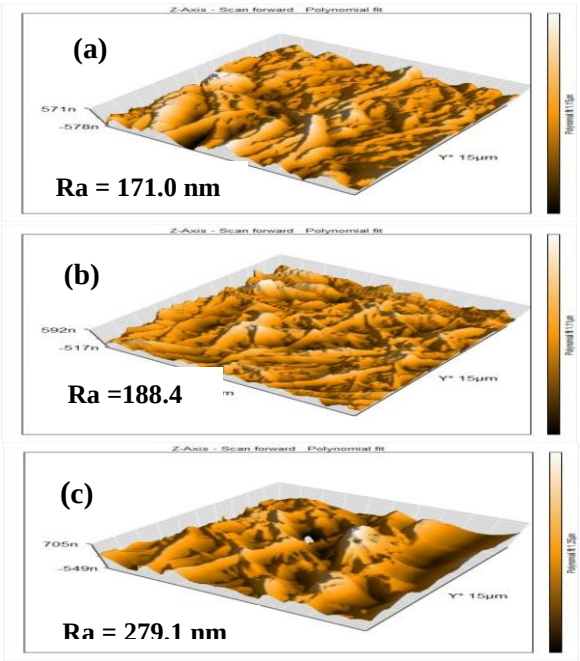

Figure 3. Microphotographs and evaluation of surface roughness of the electrospun membranes were carried out with PVDF contents of DMF solvent: (a) 10 wt.%, (b) 12 wt.%, and (c) 14 wt.%.

3.3. Wettability and porosity of membranes

In Fig. 4, the electrospun PVDF membrane's average contact angle values are documented along with surface roughness images for all the differing precursor solution concentrations of 10%, 12%, and 14% solvents (DMF).The contact angle recorded was around 81°, 87°, and 135° for PVDF concentrations of 10, 12, and 14 weight percent in DMF, respectively. Additionally, all samples show membranes formed of PVDF in DMF, which, as expected, exhibit high contact angle values, revealing their hydrophobic nature. Furthermore, it was noted that the 14 wt.% PVDF/DMF membrane had the highest contact angle value of 135°. This may be attributed to lower beads forming and greater surface roughness. These results seem to be based on experimental results often reported in the literature [34].

Additionally, Fig. 4 shows surface roughness and contact angle relationships for the pristine electrospun PVDF/DMF membrane. This is done for different values of precursor solution concentration, where the relationship demonstrated a positive trend. It was clear that changes in the contact angle of this membrane were linked to its surface characteristics; therefore, the degree of roughness affects contact angles [33].

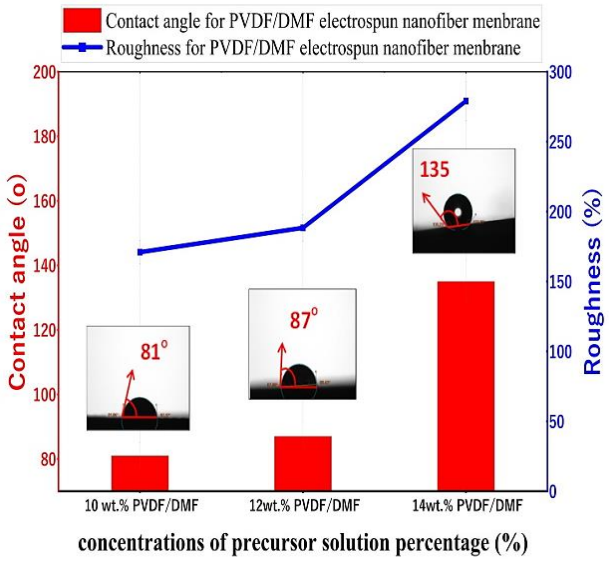

Figure 4. Measured surface roughness and specific contact angle values at several precursor solution concentrations with images.

Fig. 5 shows the inverse relationship between porosity and fiber thickness in PVDF-based nanofibrous structures. As indicated before, raising the precursor solution concentration results in a greater fiber thickness. Therefore, the increment in porosity from 73 to 76%, which was noted, is remarkably above that of the rest of the PVDF-based nanostructured membranes, and this might be related to the increased thickness of the fibers in the membranes.

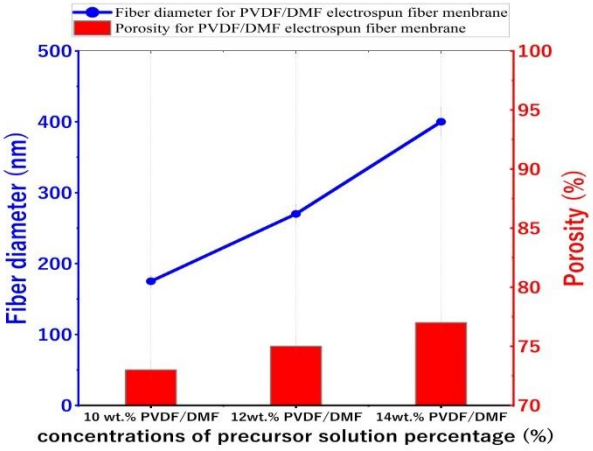

Figure 5. The porosity and fiber diameter of the electrospun PVDF nanofiber membranes were investigated at different precursor solution concentrations

3.4. Membrane performance results

As shown in Fig. 6, the separation performance test was carried out with electrospun PVDF-based nanofiber membranes synthesized with a precursor solution concentration of 10 wt.%, 12 wt.%, and 14 wt.% using DMF as solvent. The permeate flow rate and oil removal efficiency achieved were 58, 91, and 136 LMH, respectively, while the rejection rates were 85.5%, 93.9%, and 96%.

Additionally, the 14 wt.% polymeric PVDF nanofiber membrane performed best regarding permeate flow and oil removal, achieving maximums of 136 LMH and 96%, respectively. This is due to its higher porosity, which decreases the transmembrane resistance and enhances the membrane's permeate flux [35].

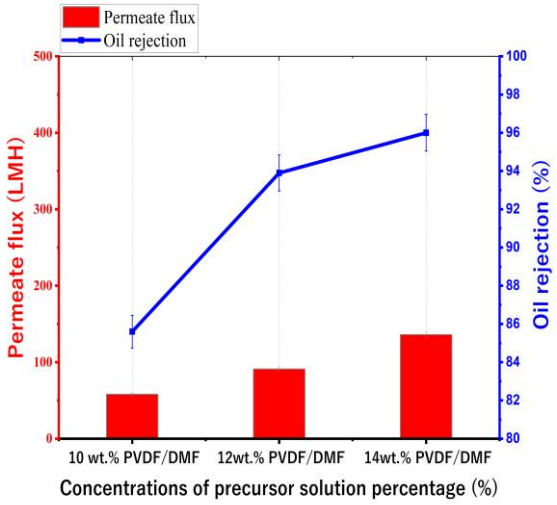

Figure 6. Separation efficiency of electrospun nanofiber PVDF-based membranes synthesized with various concentrations of precursor solutions.

4. Conclusion

Based on the results and discussion presented in the work, it is derivable that different levels of the initial mixture containing PVDF affected the morphological features, topography, wettability, porosity, and separation performance of PVDF/DMF electrospun nanofiber membranes. The concentration of the precursor solution is positively correlated with its nanofiber diameter, surface roughness, and contact angle values, showing improved water–repellent characteristics of the membranes.

It was found that an increase in fiber diameter corresponded with an augmentation of membrane porosity. The highest separation performance was observed for the 14% PVDF-based nanofiber membrane; obtaining a permeate flux of 136 LMH and 96% oil rejection is remarkable without applying any pressure. The study provides valuable insights into designing and optimizing PVDF/DMF electrospun nanofiber membranes for various applications, including oil-water separation. Future studies should focus on comparing this membrane with another polymeric membrane, incorporating nanomaterials, and conducting large-scale testing in industrial applications to improve its performance further.

Conflict of interest

The authors confirm that the publication of this article causes no conflict of interest.

Author Contribution Statement

Thamer Diwan conducted the formal analysis, investigation, and data curation and was responsible for writing the original draft.

Zaidun N. Abudi developed the methodology for the study.

Mustafa H. Al-Furaiji conceptualized the study and contributed to the manuscript's writing, review, and editing.

Zaidun N. Abudi and Mustafa H. Al-Furaiji provided joint supervision for the project.

All authors have read and agreed to the published version of the manuscript.

References

[1] B. Mishra, P. Kumar, C. Saraswat, S. Chakraborty, and A. Gautam, "Water Security in a Changing Environment: Concept, Challenges, and Solutions," *Water*, vol. 13, no. 4, p. 490, Feb. 2021, doi: https://doi.org/10.3390/w13040490.

[2] W. Ma *et al.*, "Electrospun fibers for oil-water separation," *RSC Advances*, vol. 6, no. 16, pp. 12868–12884, 2016, doi: https://doi.org/10.1039/C5RA27309A.

[3] I. S. Chronakis, "Novel nanocomposites and nanoceramics based on polymer nanofibers using electrospinning process—A review," *Journal of Materials Processing Technology*, vol. 167, no. 2–3, pp. 283–293, Aug. 2005, doi: https://doi.org/10.1016/j.jmatprotec.2005.06.053.

[4] X. Wang and B. S. Hsiao, "Electrospun nanofiber membranes," *Current Opinion in Chemical Engineering*, vol. 12, pp. 62–81, May 2016, doi: https://doi.org/10.1016/j.coche.2016.03.001.

[5] T. Al-Jadir *et al.*, "Fabrication and Characterization of Polyphenylsulfone/Titanium Oxide Nanocomposite Membranes for Oily Wastewater Treatment," *Journal of Ecological Engineering*, vol. 23, no. 12, pp. 1–13, 2022, doi: https://doi.org/10.12911/22998993/154770.

[6] R. Wahi, L. A. Chuah, T. S. Y. Choong, Z. Ngaini, and M. M. Nourouzi, "Oil removal from aqueous state by natural fibrous sorbent: An overview," *Sep Purif Technol*, vol. 113, no. 113, pp. 51–63, Jul. 2013, doi: https://doi.org/10.1016/j.seppur.2013.04.015.

[7] N. H. Barbhuiya and S. P. Singh, "Membrane Technology for Desalination and Wastewater Recycling," in *Energy, Environment, and Sustainability*, 2021, pp. 137–156. doi: https://doi.org/10.1007/978-981-16-0858-2_7.

[8] A. Asad, D. Sameoto, and M. Sadrzadeh, "Overview of membrane technology," in *Nanocomposite Membranes for Water and Gas Separation*, Elsevier, 2020, pp. 1–28. doi: https://doi.org/10.1016/B978-0-12-816710-6.00001-8.

[9] H. Verweij, "Inorganic membranes," *Current Opinion in Chemical Engineering*, vol. 1, no. 2, pp. 156–162, May 2012, doi: https://doi.org/10.1016/j.coche.2012.03.006.

[10] S. Mbakop, L. N. Nthunya, and M. S. Onyango, "Recent Advances in the Synthesis of Nanocellulose Functionalized–Hybrid Membranes and Application in Water Quality Improvement," *Processes*, vol. 9, no. 4, p. 611, Mar. 2021, doi: https://doi.org/10.3390/pr9040611.

[11] Y. Liao, C.-H. Loh, M. Tian, R. Wang, and A. G. Fane, "Progress in electrospun polymeric nanofibrous membranes for water treatment: Fabrication, modification and applications," *Prog Polym Sci*, vol. 77, pp.

69–94, Feb. 2018, doi: https://doi.org/10.1016/j.progpolymsci.2017.10.003.

[12] E. Díaz-Montes and R. Castro-Muñoz, "Metabolites recovery from fermentation broths via pressure-driven membrane processes," *Asia-Pacific Journal of Chemical Engineering*, vol. 14, no. 4, Jul. 2019, doi: https://doi.org/10.1002/apj.2332.

[13] J. F. Kim, J. H. Kim, Y. M. Lee, and E. Drioli, "Thermally induced phase separation and electrospinning methods for emerging membrane applications: A review," *AIChE Journal*, vol. 62, no. 2, pp. 461–490, Feb. 2016, doi: https://doi.org/10.1002/aic.15076.

[14] S. T. Abdul-Hussein *et al.*, "Prospects of forward osmosis-based membranes for seawater mining: Economic analysis, limitations and opportunities," *Desalination*, vol. 579, p. 117477, Jun. 2024, doi: https://doi.org/10.1016/j.desal.2024.117477.

[15] J. Lin, X. Wang, B. Ding, J. Yu, G. Sun, and M. Wang, "Biomimicry via Electrospinning," *Critical Reviews in Solid State and Materials Sciences*, vol. 37, no. 2, pp. 94–114, Apr. 2012, doi: https://doi.org/10.1080/10408436.2011.627096.

[16] V. Kugarajah *et al.*, "Future applications of electrospun nanofibers in pressure driven water treatment: A brief review and research update," *Journal of Environmental Chemical Engineering*, vol. 9, no. 2, p. 105107, Apr. 2021, doi: https://doi.org/10.1016/j.jece.2021.105107.

[17] A. M. Nasir *et al.*, "Recent progress on fabrication and application of electrospun nanofibrous photocatalytic membranes for wastewater treatment: A review," *Journal of Water Process Engineering*, vol. 40, p. 101878, Apr. 2021, doi: https://doi.org/10.1016/j.jwpe.2020.101878.

[18] F. E. Ahmed, B. S. Lalia, and R. Hashaikeh, "A review on electrospinning for membrane fabrication: Challenges and applications," *Desalination*, vol. 356, pp. 15–30, Jan. 2015, doi: https://doi.org/10.1016/j.desal.2014.09.033.

[19] P. Saxena and P. Shukla, "A comprehensive review on fundamental properties and applications of poly(vinylidene fluoride) (PVDF)," *Advanced Composites and Hybrid Materials*, vol. 4, no. 1, pp. 8–26, Mar. 2021, doi: https://doi.org/10.1007/s42114-021-00217-0

[20] N. Beauregard *et al.*, "Enhancing iCVD Modification of Electrospun Membranes for Membrane Distillation Using a 3D Printed Scaffold," *Polymers (Basel)*, vol. 12, no. 9, p. 2074, 2020, doi: https://doi.org/10.3390/polym12092074

[21] H. Li, W. Shi, X. Zeng, S. Huang, H. Zhang, and X. Qin, "Improved desalination properties of hydrophobic GO-incorporated PVDF electrospun nanofibrous composites for vacuum membrane distillation," *Separation and Purification Technology*, vol. 230, p. 115889, Jan. 2020, doi: https://doi.org/10.1016/j.seppur.2019.115889

[22]]M. Obaid et al., "Under-oil Superhydrophilic Wetted PVDF Electrospun Modified Membrane for Continuous Gravitational oil/water Separation with Outstanding Flux," Water Research, vol. 123, pp. 524–535, Oct. 2017, doi: https://doi.org/10.1016/j.watres.2017.06.079

[23] C. Du, Z. Wang, G. Liu, W. Wang, and D. Yu, "One-step Electrospinning PVDF/PVP-TiO2 Hydrophilic Nanofiber Membrane with Strong oil-water Separation and anti-fouling Property," Colloids and Surfaces A: Physicochemical and Engineering Aspects, vol. 624, p. 126790, Sep. 2021, doi: https://doi.org/10.1016/j.colsurfa.2021.126790

[24] K. Venkatesh, G. Arthanareeswaran, A. C. Bose, and P. S. Kumar, "Hydrophilic Hierarchical Carbon with TiO2 Nanofiber Membrane for High Separation Efficiency of Dye and oil-water Emulsion," Separation and Purification Technology, vol. 241, p. 116709, Jun. 2020, doi: https://doi.org/10.1016/j.seppur.2020.116709

[25] B. I. Waisi, J. T. Arena, N. E. Benes, Arian Nijmeijer, and J. R. McCutcheon, "Activated Carbon Nanofiber Nonwoven for Removal of Emulsified Oil from Water," Microporous and Mesoporous Materials, vol. 296, pp. 109966–109966, Dec. 2019, doi: https://doi.org/10.1016/j.micromeso.2019.109966

[26] M. Al-Furaiji, J. T. Arena, J. Ren, N. Benes, A. Nijmeijer, and J. R. McCutcheon, "Triple-Layer Nanofiber Membranes for Treating High Salinity Brines Using Direct Contact Membrane Distillation," *Membranes*, vol. 9, no. 5, p. 60, May 2019, doi: https://doi.org/10.3390/membranes9050060.

[27] R. Jamshidi Gohari *et al.*, "A novel super-hydrophilic PSf/HAO nanocomposite ultrafiltration membrane for efficient separation of oil/water emulsion," *Separation and Purification Technology*, vol. 150, pp. 13–20, Aug. 2015, doi: https://doi.org/10.1016/j.seppur.2015.06.031.

[28] B. Chakrabarty, A. Ghoshal, and Mihir Kumar Purkait, "Crossflow ultrafiltration of stable oil-in-water emulsion using polysulfone membranes," Chemical Engineering Journal, vol. 165, no. 2, pp. 447–456, Dec. 2010, doi: https://doi.org/10.1016/j.cej.2010.09.031.

[29] Y. Cai *et al.*, "Nanofibrous metal-organic framework composite membrane for selective efficient oil/water emulsion separation," *Journal of Membrane Science*, vol. 543, pp. 10–17, Dec. 2017, doi: https://doi.org/10.1016/j.memsci.2017.08.047.

[30] N. Bhardwaj and S. C. Kundu, "Electrospinning: A fascinating fiber fabrication technique," *Biotechnology Advances*, vol. 28, no. 3, pp. 325–347, May 2010, doi: https://doi.org/10.1016/j.biotechadv.2010.01.004.

[31] A. Greiner and J. H. Wendorff, "Electrospinning: A Fascinating Method for the Preparation of Ultrathin Fibers," *Angewandte Chemie International Edition*, vol. 46, no. 30, pp. 5670–5703, Jul. 2007, doi: https://doi.org/10.1002/anie.200604646.

[32] R. Al-Attabi, Y. Morsi, W. Kujawski, L. Kong, J. A. Schütz, and L. F. Dumée, "Wrinkled silica doped electrospun nano-fiber membranes with engineered roughness for advanced aerosol air filtration," *Separation and Purification Technology*, vol. 215, pp. 500–507, May 2019, doi: https://doi.org/10.1016/j.seppur.2019.01.049.

[33] Z. Zhou and X.-F. Wu, "Electrospinning superhydrophobic–superoleophilic fibrous PVDF membranes for high-efficiency water–oil separation," *Materials Letters*, vol. 160, pp. 423–427, Dec. 2015, doi: https://doi.org/ 10.1016/j.matlet.2015.08.003.

[34] P. Nuamcharoen, T. Kobayashi, and P. Potiyaraj, "Influence of Volatile Solvents and Mixing Ratios of Binary Solvent Systems on Morphology and Performance of Electrospun poly(vinylidene fluoride) Nanofibers," Polymer International, vol. 70, no. 10, pp. 1465–1477, Apr. 2021, doi: https://doi.org/10.1002/pi.6218

[35] X. Wang, Q. Xiao, C. Wu, P. Li, and S.-Y. Xia, "Fabrication of Nanofiltration Membrane on MoS2 Modified PVDF Substrate for Excellent Permeability, Salt Rejection, and Structural Stability," Chemical Engineering Journal, vol. 416, pp. 129154–129154, Jul. 2021, doi: https://doi.org/10.1016/j.cej.2021.129154